A&A 494, 263–268 (2009)
DOI: 10.1051/0004-6361:200810662

Astronomy & Astrophysics

Two types of flare-associated coronal mass ejections

G. Michalek

Astronomical Observatory of Jagiellonian University, Cracow, Poland
e-mail: michalek@oa.uj.edu.pl

Received 23 July 2008 / Accepted 15 October 2008

ABSTRACT

Aims. Here, we study the relationship between flares and CMEs.
Methods. For this purpose a statistical analysis of 578 flare-associated CMEs is presented. We considered two types of flare-associated CMEs: CMEs that follow and precede flare onset.
Results. We shown that both samples have quite different characteristics. The first type of CMEs tends to be decelerated (median acceleration = –5.0 m s^{-2}), faster (median velocity = 519 km s^{-1}), and physically related to flares (a correlation coefficient between the energy of the CME and the peak of the X-ray flare = 0.80). The CMEs preceding associated flares are mostly accelerated (median acceleration = 5.4 m s^{-2}), slightly slower (median velocity = 487 km s^{-1}), and poorly related to flares (a correlation coefficient between the energy of the CME and the peak of the X-ray flare = 0.12).
Conclusions. These two types of flare-associated CMEs demonstrate that magnetic reconnection, which influences the CME acceleration, could be significantly different in the two types of events.

Key words. Sun: coronal mass ejections (CMEs) – Sun: flares

1. Introduction

The two most important energetic phenomena on the Sun: a flare, which is a sudden flash of electromagnetic radiation, and a coronal mass ejection (CME), which is an eruption of solar plasma into interplanetary space. CMEs and flares originate in closed magnetic fields and are different manifestations of the same process which releases magnetic free energy. The first CME was detected on December 14, 1971 by the white-light coronagraph on board NASA's seventh Orbiting Solar Observatory (Tousey 1973). From the early days of CME observations, it is well known that CMEs are associated with flares and prominences (Munro et al. 1979). Kahler (1992) showed that 40% of CMEs are associated with H-alpha flares. The CME association rate clearly increases with the peak of X-ray intensity. The CME association rate increases from 40% (M-class flares) to 90% (X-class flares) (e.g. Yashiro et al. 2006). The spatial and temporal relationship between flares and CMEs was also considered in detail (Harrison 1987; Kahler et al. 1989; Harrison 1991; Hundhausen 1999; Moon et al. 2002; Yashiro et al. 2008). These studies demonstrated that CME onset typically precedes the related X-ray flare onset by several minutes. The LASCO coronagraphs and other instruments have been used to understand the initial speed and acceleration profiles of CMEs. Zhang et al. (2004) found a three-phase acceleration profile. A slow rise over tens of minutes, followed by a rapid acceleration of 100–500 m s^{-2} occurs in the height range 1.4 to 4.5 $R_\odot$ during the flare rising phase and a propagation with constant or declining speed. Gosling et al. (1976) and MacQueen & Fisher (1983) suggested that different mechanisms could accelerate CMEs associated with prominences and flares. The rapid acceleration of CMEs is strongly correlated with the rising phase of the associated soft X-ray bursts (Zhang et al. 2004; Vršnak et al. 2004). The flare-associated CMEs are faster and decelerating, while the prominence-associated CMEs are slower and accelerating in the LASCO FOV (St. Cyr et al. 1999). In a statistical analysis of 545 flare-associated CMEs and 104 non-flare CMEs, Vršnak et al. (2005) found that both data sets have similar characteristics and form one consistent group of CMEs.

All CMEs have to be accelerated as they lift off from the surface. During the next phase of propagation a balance between propelling and retarding forces determines the dynamics of the CMEs. Recent studies demonstrate that the propelling force ceases at heights below 4 $R_\odot$ (Chen & Krall 2003). So, in the LASCO FOV, drag determines the acceleration of CMEs. This interpretation was proved by statistical analyses (Yashiro et al. 2004). Generally it is assumed that fast CMEs ($V \geq 900$ km s^{-1}) are decelerated and slow CMEs ($V \leq 400$ km s^{-1}) are accelerated by the drag force (Yashiro et al. 2004). In the present study we consider statistical properties of the flare-associated CMEs only. To perform a detailed study we separate these events into two groups: CMEs following and preceding the associated flares.

The paper is organized as follows: in Sect. 2, the data considered in the study is described. In Sect. 3, we perform a broad statistical analysis of the flare-associated CMEs. Discussion and conclusions are presented in Sect. 4.

2. Data

We describe a procedure used to compile the list of events employed in the study. For our analysis we use two data sets – CMEs and flares. A full description of CMEs in the range of 2–30 solar radii is included in the SOHO/LASCO catalog. We considered all CMEs detected from the beginning of 2000 until the end of 2004. Next, using data from the geosynchronous operating environmental satellites (GOES), associated flares observed in soft X-ray range were determined.

For this purpose we used the database from the National Geophysical Data Center (www.ngdc.noaa.gov/stp/SOLAR/ftpsolarflares.html). X-ray observations provide an accurate detection of the start of solar flares. For the associated flare onset times, durations, source locations, moments of the peak flux and the peak fluxes were obtained. The duration of X-ray flares is defined in this database as when the current flux returns to 0.5 of the peak value. In addition the data are not background subtracted and the durations of the X-ray flares could be ambiguous. In order to associate flares with CMEs we employed temporal and spatial criteria. Using the height-time plots we determined onset times (T_o, from quadratic fit) of CMEs. We assume that a given flare is related to a given CME if it appears 100 min before or after associated CMEs (a onset of an associated flare should be in a time window ±100 min with respect to T_o). Additionally we required that the location of flares is in the same quadrant of the Sun as the associated CMEs. Using our criteria we found the 578 flare-associated CMEs during 2000–2004. In our work we consider two samples of flare-associated CMEs: those starting before (BF-CMEs) or after associated flares (AF-CMEs). As we mentioned, the onset times of CMEs are determined from back extrapolations of the height-time plots and are subject to errors of up to several minutes. To accurately separate CMEs into the two sets of events we excluded these pairs of CMEs and flares which had almost the same onset times (in a time window ±5 min). In this way we established a sample of the 439 flare-associated CMEs used for further considerations.

3. Results

In the considered period, 2000–2004, we recorded the 283 CMEs starting before and 156 starting after the associated flares. In the next subsections we present a statistical analysis of these samples of CMEs.

3.1. The acceleration of CMEs

Figure 1 shows the acceleration distributions for all the considered CMEs (top panel), the AF-CMEs (middle panel) and the BF-CMEs (bottom panel). The average acceleration of the all CMEs is slightly negative (median = -2.0 m s^{-2}). This tendency is due to the CMEs following the associated flares. These events are clearly decelerated (median = -5.0 m s^{-2}) and more populated than the CMEs preceding the flares. On the other hand the CMEs that precede the flares are obviously accelerated (median = 5.4 m s^{-2}). Generally it is assumed (Chen & Krall 2003; Yashiro et al. 2004) that in the LASCO FOV, the dynamics of CMEs is determined by drag which depends on the difference between velocities of CMEs and the interplanetary medium. Before we drow any final conclusions about dynamics of the flare-associated CMEs it is necessary to consider the kinematic properties of the samples of CMEs.

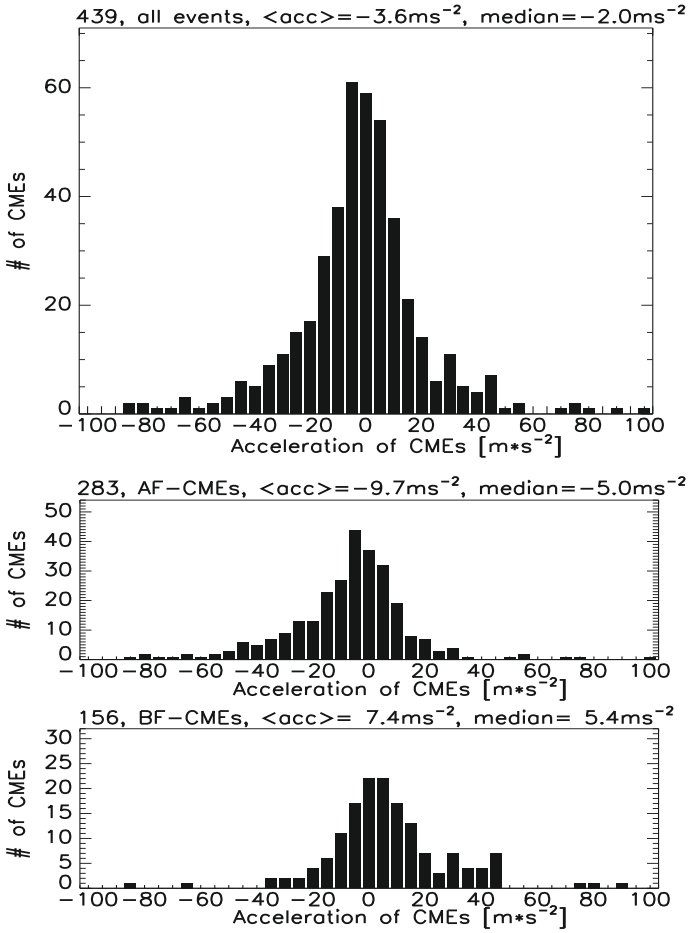

Fig. 1. The acceleration distribution of the all CMEs (*top panel*), the AF-CMEs (*middle panel*) and the BF-CMEs (*bottom panel*).

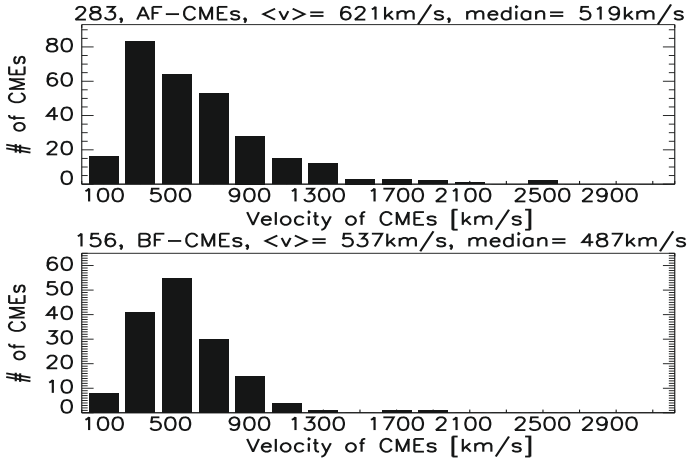

Fig. 2. The velocity distributions of the AF-CMEs (*top panel*) and the BF-CMEs (*bottom panel*).

3.2. The velocity and energy of CMEs

Figure 2 shows the velocity distributions of the AF-CMEs and BF-CMEs. There are no significant differences between velocities of the two samples of events. The AF-CMEs seem to be slightly faster (median = 519 km s^{-1}) than the BF-CMEs (median = 487 km s^{-1}). The difference is too small to explain the acceleration behavior of both categories of events by drag. On average both categories of flare-associated CMEs are faster than the whole population of CMEs (Yashiro et al. 2004, $\langle V \rangle$ = 489 km s^{-1}). According to the results presented in Yashiro et al.'s paper both categories of CMEs should be slightly decelerated. Not only the velocity but also the kinetic energy of CMEs is important when we consider the influence of drag on their acceleration. The AF-CMEs ($\langle$kinetic energy$\rangle$ = 2.44^{31} erg) are more energetic than the BF-CMEs ($\langle$kinetic energy$\rangle$ = 6.25^{30} erg). It is interesting that the more energetic AF-CMEs tend to be so significantly decelerated. Figure 3 shows the energy of CMEs versus the peak flux of X-ray flares. The AF-CMEs seem to

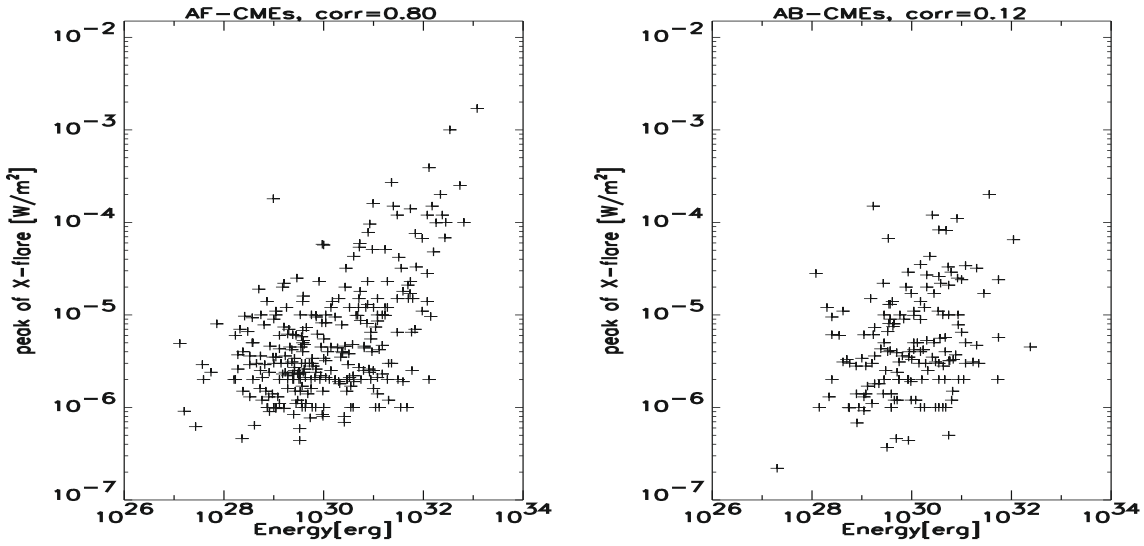

Fig. 3. The scatter plots of the energy of CMEs versus the peak flux of X-ray flares of the AF-CMEs (*left panel*) and BF-CMEs (*right panel*).

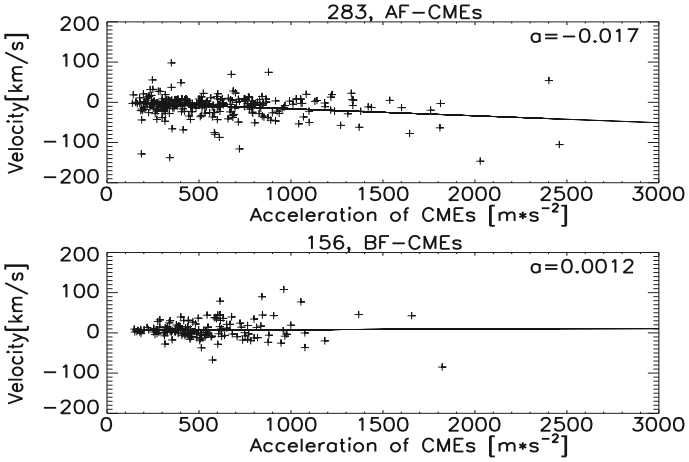

Fig. 4. The acceleration-velocity relationships of the AF-CMEs and BF-CMEs. Continuous lines represent linear fits to the data points. In the right top corners there are coefficients describing the slope of the linear functions.

be physically related to the associated flares (a correlation coefficient between the energy of CME and the peak of X-ray flare = 0.80). The BF-CMEs are poorly related to the flares (a correlation coefficient between the energy of CMEs and the peak of X-ray flare = 0.12).

3.3. The velocity-acceleration relationship

Figure 4 shows the acceleration-velocity relationships of the AF-CMEs and BF-CMEs. Continuous lines represent linear fits to the data point. The AF-CMEs show an anti-correlation of the acceleration and velocity (the slope coefficient of a linear fit = –0.0172), consistent with that obtained by Yashiro et al. (2004) and Vršnak et al. (2004). The second sample of CMEs (the BF-CMEs) does not show a similar trend (the slope coefficient of a linear fit = 0.0012). This behavior is inconsistent with the aerodynamic drag interpretation. This is surprising and means that these events are subjected to the prolonged action of the driving force in the LASCO FOV. Figure 5 shows the acceleration distributions of the CMEs with velocities ranges within $V < 400$ km s^{-1} (top panels), 400 km s^{-1} $\leq V \leq$ 800 km s^{-1} (middle panels) and $V > 800$ km s^{-1} (bottom panels). The left and right panels show the CMEs starting after and before the associated flares, respectively. The figures show again that the AF-CMEs are mostly decelerated but the BF-CMEs tend to be accelerated. These trends do not depend on the velocities of CMEs. Depending on the velocity range, the AF-CMEs have median decelerations from –2.5 m s^{-2} (for the slowest CMEs) to –10 m s^{-2} (for the fastest ones). On the other hand, the BF-CMEs have median accelerations from 7.0 m s^{-2} (for the slowest CMEs) to 5.5 m s^{-2} (for the fastest ones). Two panels present the most interesting results. The top left panel shows that even the slowest ($V < 400$ km s^{-1}) AF-CMEs are decelerated (median = −2.5 m s^{-2}). Yashiro et al. (2004) demonstrated that in this velocity range the whole population of CMEs tend to be accelerated (median = 1.6 m s^{-2}). Secondly, the right bottom panel indicates that the fastest ($V > 800$ km s^{-1}) BF-CMEs tend to be accelerated (median = 5.5 m s^{-2}). Yashiro et al. (2004) presented that in a similar velocity range ($V > 900$ km s^{-1}) the whole population of CMEs tends to be decelerated (median = −16 m s^{-2}). It is interesting that even the slowest AF-CMEs tend to be decelerated and the fastest BF-CMEs tend to be accelerated. Such results are inconsistent with the aerodynamic drag interpretation.

3.4. Temporal relationship between flares and CMEs

In our study we assumed that the flares and CMEs are physically associated if both phenomena appear in the time window ±100 min. Figure 6 shows the distribution of the difference time (ΔT) between the onsets of CMEs and flares. In the figure we show 578 events because we did not exclude, as in the previous considerations, the associated events originating in a time window ±5 min. The distribution of ΔT is almost symmetric and Gaussian. About 80% of the associated phenomena have ΔT lower than ±30 min. We repeated the same studies (the same plots) as in previous subsections but choosing lower limits for ΔT (±60 min, ±30 min and including events having almost the

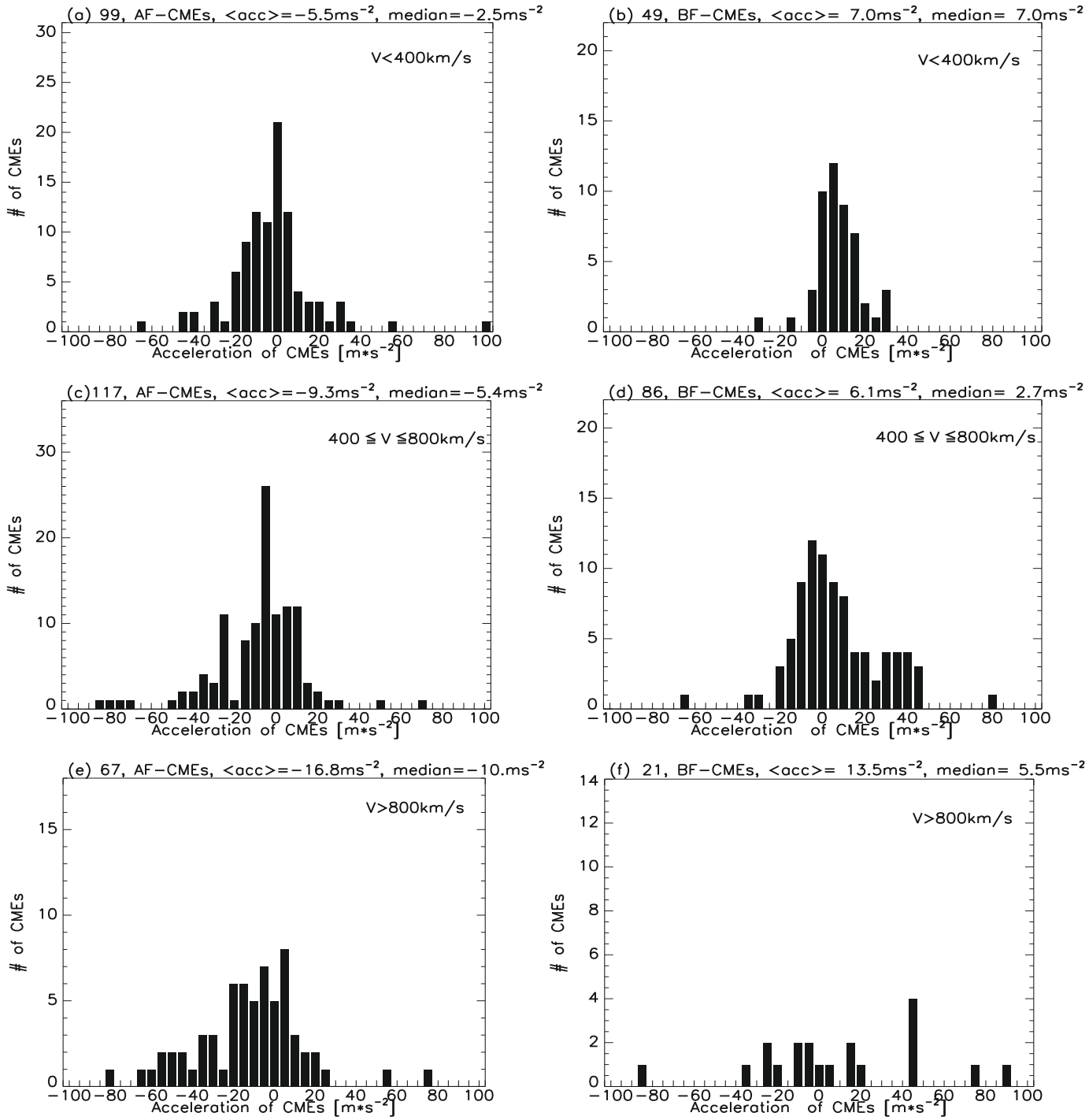

Fig. 5. The acceleration distributions of the CMEs with the velocities ranges within $V < 400$ km s^{-1} (panels **a**), **b**)), 400 km s^{-1} $\leq V \leq$ 800 km s^{-1} (panels **c**), **d**)) and $V > 800$ km s^{-1} (panels **e**), **f**)). *Left and right panels* show the AF-CMEs and BF-CMEs, respectively.

same onset times ±5 min). We obtained almost the same results (trends) as were presented in the previous sections. We only observed that CMEs which were more temporally related to the associated flares were slightly faster (on average by about 50 km s^{-1} for CMEs that appeared in the time window ±30 min with respect to the associated flares). The results presented in the previous subsections do not depend on temporal linking between the flares and CMEs. Additionally, in Fig. 7 the diofstributions X-ray fluxes of flares associated with the two types of CMEs are presented. Both categories of CMEs are associated with similar populations of X-ray flares.

3.5. The velocity-width relationship

Figure 8 shows the velocity-width relationships of the AF-CMEs and BF-CMEs. There is a poor correlation between these parameters for the AF-CMEs (0.44) and the BF-CMEs (0.30). In the figures we also presented halo CMEs (width = 360°) but they were not included in the calculations of the correlation coefficients and average widths. Both categories of CMEs have similar average widths (⟨AF-CMEs width⟩ = 69°, and ⟨BF-CMEs width⟩ = 72°) but in the case of the AF-CMEs we observed many more halo CMEs.

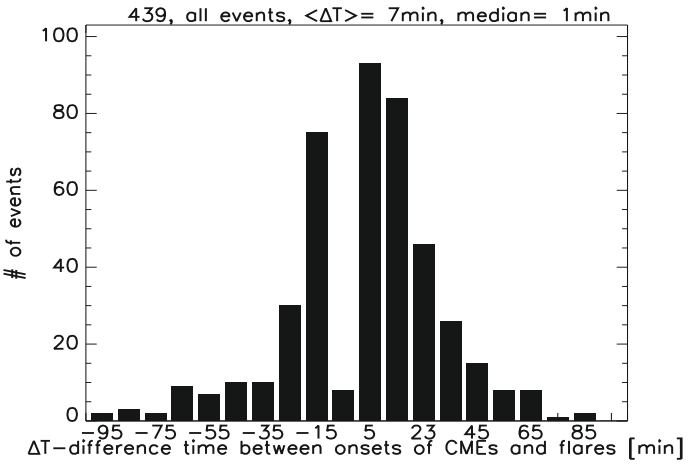

Fig. 6. The distribution of the difference times between the onsets of CMEs and flares (ΔT = CMEs onset time – flare onset time).

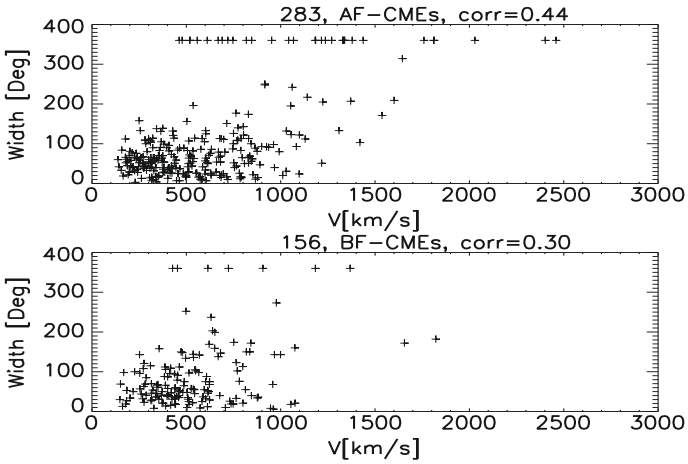

Fig. 8. The velocity-width relationship of the AF-CMEs (*top panel*) and BF-CMEs (*bottom panel*).

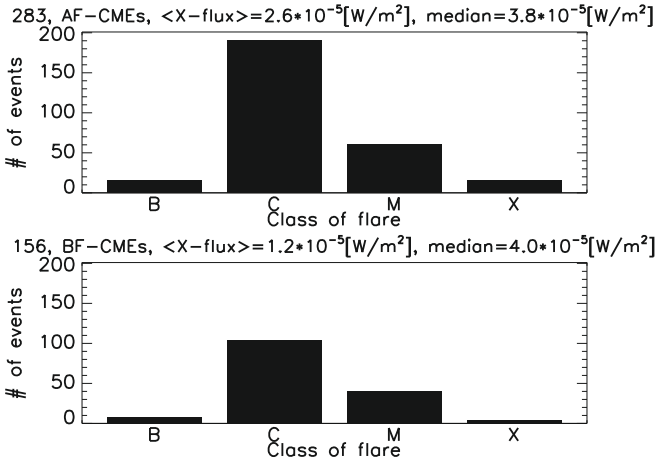

Fig. 7. The distribution of X-ray flares associated with the AF-CMEs (*top panel*) and BF-CMEs (*bottom panel*).

4. Summary and discussion

In the present paper we considered the flare-associated CMEs observed during 2000–2004. We separately studied the two samples of CMEs: the CMEs following (AF-CMEs) and preceding (BF-CMEs) the associated flares. The CMEs after the associated flares tend to be decelerated (median acc = $-5.5\ \mathrm{m\,s^{-2}}$). This trend is independent of the velocity of the CMEs (Figs. 4 and 5), even the slowest events ($V < 400\ \mathrm{km\,s^{-1}}$) are mostly decelerated (median acc = $-2.5\ \mathrm{m\,s^{-2}}$). Such a behavior (except deceleration for the slowest events) was also observed in previous works (Yashiro et al. 2004; Vršnak et al. 2005). These events seem to be accelerated during the rising phase of flares and in the LASCO FOV the speed is determined by the drag force of the interplanetary medium. The AF-CMEs are slightly faster then the BF-CMEs and they are strongly related to the flares. The correlation coefficient between the energy of CMEs and the peak of X-ray fluxes is 0.80. The correlation is so significant because the AF-CMEs receive the total propelling energy in the beginning phase of propagation (in the LASCO FOV). The energy is transported by the upward-directed reconnection jets which enhance and prolong the flux rope acceleration until the associated X-ray flares are in the increasing phase of eruption (Mouschovias & Poland 1978; Chen 1989; Vršnak 1990; Cheng et al. 2003). Probably in the case of the slowest events, the reconnection does not generate such jets but only reduces the magnetic tension and diminishes the erupting-flux rope acceleration (e.g. Anzer & Pneuman 1982; Cheng & Krall 2003; Lin et al. 2004). These events tend to be decelerated even if they are slow (Fig. 5, top left panel).

The BF-CMEs are significantly different. They tend to be accelerated in the LASCO FOV. This trend is independent of the velocities of the CMEs. Even the fastest ($V > 800\ \mathrm{km\,s^{-1}}$) CMEs also have the tendency to be accelerated. The BF-CMEs have a delayed propelling boost (due to the flare reconnection process) when the associated flares start in the later phase of propagation. In the case of these CMEs the flare boosting Lorentz force is delayed with respect to the onset of the CME. These events are slightly slower in comparison to the AF-CMEs (but slightly faster than the total population of CMEs) and they seem to be poorly related to the associated flares. The correlation coefficient between the CME energy and the peak of the X-ray flux is only 0.12. Probably these events have the similar "flare hoop-force" as the AF-CMEs but it is delayed (starts when the associated X-ray flares appear). The correlation between these parameters might be more significant if we could observe the CMEs behind the LASCO FOV until the propelling force ceases. The BF-CMEs are a specific type of event triggering X-ray flares (during propagation through the corona) which causes the "second step" acceleration of these events.

Considerations of the lower limits of ΔT proved that these trends (for both categories of CME) do not depend on a temporal relation between the associated flares and CMEs.

X-ray observations provide an accurate detection of the start of solar flares. The situation is different in the case of the onset times of CMEs. These times are received from back extrapolations of the height-time plots to the surface of the Sun. The onset times of CMEs are subject to errors for two reasons. First, the height-time plots are obtained through subjective manual measurements from LASCO coronagraphic images. So, the height-time plots strongly depend on the quality (especially brightness) of a particular event. Additionally, linear or quadratic fits used for the back extrapolations give only the approximate onset times of CMEs. The both kinds of errors are very difficult to estimate. To minimize errors three precautions were taken. First, we considered a large sample of events (to increase the statistics). To obtain the more accurate onset times for the back extrapolations quadratic fits were used. Additionally, we excluded associated

events that started almost at the same time (in the time window ±5 min).

We studied the dynamics of CMEs in the 2–30 $R_\odot$ range. So, we cannot exclude that the two categories of flare-associated CMEs have different initiation mechanisms.

Acknowledgements. Work done by Grzegorz Michalek was supported by *MNiSW* through the grant N203 023 31/3055. In the paper we used data from the SOHO/LASCO catalog. This CME catalog is generated and maintained at the CDAW Data Center by NASA and The Catholic University of America in cooperation with the Naval Research Laboratory. SOHO is a project of international cooperation between ESA and NASA.

References

Anzer, U., & Pneuman, G. W. 1982, Sol. Phys., 79, 129
Chen, J. 1989, ApJ, 338, 453
Chen, J., & Krall, J. 2003, J. Geophys. Res., 108, 1410
Cheng, C. Z., Ren, Y., Choe, G. S., & Moon, Y. J. 2003, ApJ, 596, 1341
Gosling, J. T., Hildner, E., MacQueen, et al. 1976, Sol. Phys., 48, 389
Harrison, R. A. 1987, A&A, 182, 337
Harrison, R. A. 1991, Adv. Space Res., 11, 25
Hundhausen, A. 1999, Coronal Mass Ejections, in The Many Faces of the Sun: a summary of the results from NASA's SMM, ed. K. T. Strong, et al. (New York: Springer), 104
Kahler, S. W. 1992, ARA&A, 30, 113
Kahler, S. W., Sheeley, N. R., & Liggett, M. 1989, ApJ, 344, 1026
Lin, J., Raymond, J. C., & van Ballegooijen, A. A. 2004, ApJ, 602, 422
MacQueen, R. M., & Fisher, R. R. 1983, Sol. Phys., 89, 89
Mouschovias, T. Ch., & Poland, A. I. 1978, ApJ, 220, 675
Moon, Y.-J., Choe, G. S., Wang, H., et al. 2002, ApJ, 581, 694
Munro, R. H., Gosling, J. T., Hildner, E., et al. 1979, Sol. Phys., 61, 201
St. Cyr, O. C., Burkepile, J. T., Hundhausen, A. J., & Lecinski, A. R. 1999, J. Geophys., Res., 104, 12493
Tousey, R. 1973, in Space Research XIII, ed. M.J., Rycroft, & S. K., Runcorne (Berlin: Akademie-Verlag), 713
Vršnak, B. 1990, Sol. Phys., 129, 295
Vršnak, B., Ruždjak, D., Sudar, D., & Gopalswamy, N. 2004, A&A, 423, 717
Vršnak, B., Sudar, D., & Ruždjak, D. 2005, A&A, 435, 1149
Yashiro, S., Gopalswamy, N., Michalek, G., et al. 2004, J. Geophys. Res., 109, CiteID A07105
Yashiro, S., Akiyama, S., Gopalswamy, N., & Howard, R. A. 2006, ApJ, 650, 438
Yashiro, S., Michalek, G., Akiyama, S., Gopalswamy, N., & Howard, R. A. 2008, ApJ, 673, 1174
Zhang, J., Dere, K. P., Howard, R. A., & Vourlidas, A. 2004, ApJ, 604, 420